



Implications of ab initio energetics on the thermodynamics of Fe–Cr alloys

A. Caro, M. Caro, E. M. Lopasso, and D. A. Crowson

Citation: [Applied Physics Letters](#) **89**, 121902 (2006); doi: 10.1063/1.2354445

View online: <http://dx.doi.org/10.1063/1.2354445>

View Table of Contents: <http://scitation.aip.org/content/aip/journal/apl/89/12?ver=pdfcov>

Published by the [AIP Publishing](#)

Articles you may be interested in

[The Bain path of paramagnetic Fe-Cr based alloys](#)

J. Appl. Phys. **110**, 013708 (2011); 10.1063/1.3603024

[Ab initio spectroscopic characterization of the HNNO and ONHN radicals](#)

J. Chem. Phys. **134**, 084308 (2011); 10.1063/1.3556990

[Systematic ab initio calculations on the energetics and stability of covalent O 4](#)

J. Chem. Phys. **120**, 10084 (2004); 10.1063/1.1729923

[Accurate ab initio study of the energetics of phosphorus nitride: Heat of formation, ionization potential, and electron affinity](#)

J. Chem. Phys. **118**, 8290 (2003); 10.1063/1.1565317

[Gas phase ion chemistry and ab initio theoretical study of phosphine. I](#)

J. Chem. Phys. **107**, 1491 (1997); 10.1063/1.474502



Re-register for Table of Content Alerts

Create a profile.



Sign up today!



Implications of *ab initio* energetics on the thermodynamics of Fe–Cr alloys

A. Caro^{a)} and M. Caro

Chemistry and Materials Science Directorate, Lawrence Livermore National Laboratory,
Livermore, California 94550

E. M. Lopasso

Centro Atómico Bariloche—Instituto Balseiro, 8400 Bariloche, Argentina

D. A. Crowson

Virginia Polytechnic Institute and State University, Blacksburg, Virginia 24061

(Received 5 March 2006; accepted 26 July 2006; published online 18 September 2006)

The authors analyze the implications of the recently reported results of *ab initio* calculations of formation energies of the Fe–Cr alloy. The formation energies show a change in sign from negative to positive as Cr composition increases above $\sim 10\%$. By developing a classic potential to evaluate the thermodynamic properties, they determine the location of the solubility limit and compare it with earlier results. A significant difference appears in a region of temperature and composition that is relevant for the nuclear applications of this alloy. Experimental results seem to confirm the validity of the location of the new *solvus* line. © 2006 American Institute of Physics.

[DOI: 10.1063/1.2354445]

Fe–Cr ferritic martensitic steels are materials of interest for nuclear applications due to their high strength at elevated temperatures and resistance to radiation damage and corrosion. The binary Fe–Cr alloy is a model system in which the basic mechanisms of radiation damage are studied with particular emphasis these days. Fe–Cr represents a challenge for computational materials science because the magnetism in both elements combines in a complex way in the alloy. There is agreement between different sources for the phase diagram at high temperatures, see, for example, Massalsky and CALPHAD (CALculation of PHase Diagrams) diagrams,^{1,2} both based on an ensemble of experimental data, the latter, in particular, based on the results of Anderson and Sunderman.³ However, at low temperature, within the ferromagnetic (FM) phase, the situation is more uncertain. The location of the *solvus* and the invariant line (where all three phases α , α' , and σ coexist) as well as the heat of formation (hof) are under discussion. Suffice it here to say that in Ref. 1 the data below 1000 K are drawn in dashed lines, indicating the absence of accurate experimental information.

Mirebeau *et al.*⁴ reported experimental results on aged dilute Fe rich alloys that show the existence of short range order at 700 K for alloys with Cr content below 10 at. %, while segregation appeared for higher concentrations. Kuwano and Hamaguchi⁵ reported neutron irradiation results showing precipitation of Cr in the postirradiation annealing for $x_{\text{Cr}} \geq 10\%$ at 800 K. Sagaradze *et al.*⁶ reported electron irradiation results at the same temperature showing similar behavior. Inversion of the sign of short range order was recently confirmed by Shabashov *et al.*⁷ Finally, Mathon *et al.*⁸ studied steels with 7–10 wt % Cr under neutron irradiation and again confirmed the separation into α and α' . From the experimental point of view it seems clear then that both the binary alloy and the steel have ordering for low Cr content and segregation above it, a somehow interesting behavior.

Theoretical predictions of a change in sign of the hof of the alloy started with the work of Hennion,⁹ who predicted it

to be at 25% Cr. More recently Olsson *et al.*¹⁰ predicted a change in sign at 6% Cr and Mirzoev *et al.*¹¹ analyzed in more detail the origin of the change in sign of the hof in terms of the changes in the magnetic structure. Finally, Klaver¹² offers an interpretation in terms of the antiferromagnetic alignment of the Cr substitutional solute atoms and frustration effects as Cr content increases. It is then a fact that the assessed phase diagrams, as those in Refs. 1 and 2, do not have the detailed information of the anomaly in the hof at low Cr concentration. The aim of this work is to use this information about the change in sign of the hof to determine its implications regarding the location of the *solvus*. We characterize this system thermodynamically and determine the modifications to the low temperature region of the phase diagram of Fe–Cr, a region of utmost interest for nuclear applications.

To go from *ab initio* energetics to phase diagrams, the usual approach is to make approximations for the energetics of disordered configurations, like the cluster expansion method, and to assume harmonic or quasiharmonic approximations for the vibrational entropy. We instead make an approximation that consists of creating a classic potential that reproduces the energetics and several other quantities, and with it we calculate free energies with no further approximations, i.e., exact within numerical errors. The advantage of this approach is that we get a well characterized classic potential that can be later used in molecular dynamics simulations.

To determine the location of the *solvus* from the *ab initio* energetics, we use our recently developed classic potential for this alloy, based on the Fe potential reported in Ref. 13 and the Cr potential reported in Ref. 14, that reproduces static and dynamic properties quite satisfactorily.¹⁵ The free energy calculations are then performed using a thermodynamic package that we developed for this purpose, and is reported in detail in Refs. 16–20. The Embedded Atom Model potential so developed reproduces the *ab initio* hof reported in Ref. 10 and, as we show here, also gives an excess vibrational entropy in good agreement with

^{a)}Electronic mail: caro2@llnl.gov

TABLE I. Values of the Redlich-Kister expansion coefficients L_p corresponding to the hof from Ref. 10 (in eV) and values of the coefficients h_i in the polynomial expression of the cross potential (see text).

L_0	L_1	L_2	L_3	L_4
0.415 66	0.081 413 4	-0.010 189 9	0.267 659	-0.248 269
h_0	h_1	h_2	h_3	h_4
1.045 384	-0.878 122	2.130 654	-2.333 204	0.918 932

CALPHAD values.² It is different from standard EAM potentials in that the cross pair term depends on both distance and local composition. We calculate Gibbs free energies for the random solid solution and liquid phases at several values of composition and temperature $G(x, T)$. Subsequently we generate a database in the THERMOCALC format and obtain the phase diagram from this software package.² The target hof of the bcc FM solid solution is taken from Olsson *et al.*,¹⁰ which fit with a Redlich-Kister expansion to fourth order in $(1-2x)$ as $\Delta h = x(1-x)\sum_0^4 L_p(1-2x)^p$, with x the Cr composition and parameters L_p given in Table I.

The cross potential is given by $V_{AB}(x, r) = h(x)\frac{1}{2}(V_{AA}(r) + V_{BB}(r))$ with parameters in the polynomial $h(x)$ given in Table I. Figure 1 shows that the target function and the predicted value of the hof perfectly overlap. Also in Fig. 1 we show the hof of the FM phase at low T as it appears in SSOL, the database of THERMOCALC. Two discrepancies are readily observable. (i) At low Cr composition, the SSOL data show no change in sign, as has been previously discussed. (ii) The hof at all compositions above 20% is greater in the *ab initio* result (with a maximum at ~ 100 meV/at.) than in SSOL (with its maximum at ~ 60 meV/at.). This is a point of conflict because such a difference would alter the phase diagram around equiatomic composition where the σ phase exists, and the solubility limit of α' . However, three independent *ab initio* calculations¹⁰⁻¹² agree on a value of about 100 meV/at. at 50% Cr, perhaps reflecting limitations in the magnetic structure considered or finite size effects in the *ab initio* calculations. This point requires further investigation but does not invalidate our study of the low Cr content

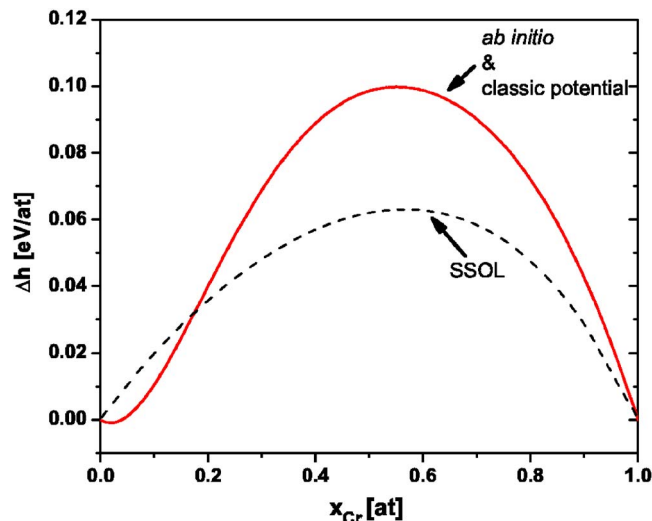


FIG. 1. (Color online) Heat of formation from Ref. 14 and predicted by the classic potential (solid line) and from SSOL (Ref. 2) (dashed line).

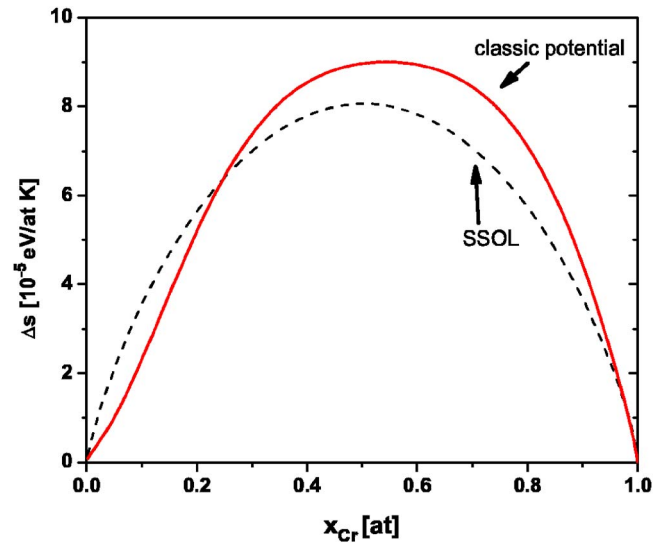


FIG. 2. (Color online) Predicted excess vibrational entropy of mixing obtained from our potential (solid line) and values of SSOL (Ref. 2) (dashed line) at low T in the ferromagnetic phase.

region of the phase diagram, where the influence of the change in sign dominates the outcome.

As a test of our approach we report in Fig. 2 the excess vibrational entropy of mixing, as obtained from the free energies of both our potential and the FM phase in SSOL database.² The agreement is good considering the fact that this quantity is not used in the development of the potential; it comes out as a prediction. We note here that despite the fact that the empirical potential does not contain any explicit degree of freedom of magnetic origin, in the FM phase that contribution to entropy is zero and therefore FM is the only phase where we should expect agreement between a classic potential and the real material.

With these free energies we get the phase diagram. Figure 3 reports the low T -low x region of interest $0 \text{ K} < T < 1000 \text{ K}$ and $0\% < x_{\text{Cr}} < 20\%$. A continuous followed by a dotted line is our results for the *solvus* in the FM phase, while the dashed line is the *solvus* as it appears in SSOL.² Our *solvus* is plotted with a solid line only for temperatures below the invariant line suggested by the experiments of Ref.

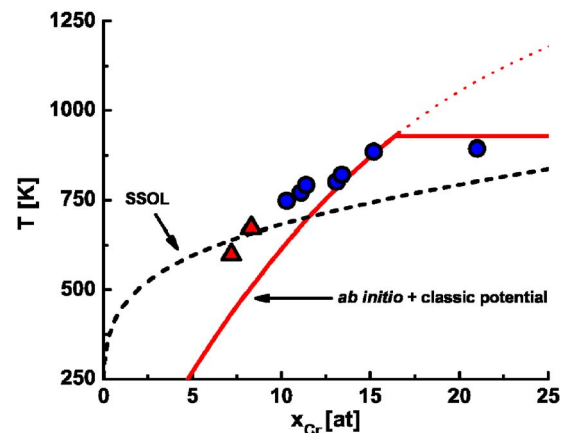


FIG. 3. (Color online) Low temperature and composition region of the phase diagram based on *ab initio* results from Ref. 14 generated using the Fe-Cr empirical potential (solid and dotted lines); *solvus* from SSOL (Ref. 2) (dashed lines); and experimental results from Ref. 5 (circles) and from Ref. 8 (triangles).

5, that we report in the figure as a horizontal solid line; above it, the *solvus* is shown with a dotted line, indicating that other effects determine the diagram at those T - x values, namely, the σ phase and the magnetic transition. In Fig. 3 we have added the experimental results of Kuwano and Hamaguchi,⁵ and those of Mathon *et al.*⁸ The discrepancy between the SSOL *solvus* and the *solvus* implied in the *ab initio* results is obvious, as is the agreement between the experimental results and our prediction. The most striking difference is the fact that the *solvus* line, if extrapolated to zero temperature, does not cross the x axis at $x=0$, as explicitly assumed in the CALPHAD treatment. This fact can easily be understood if one considers a very low T , where excess free energy is essentially equal to the excess heat of formation; then the solid line in Fig. 1 can be reinterpreted as a free energy curve and the common tangent construction would show that the miscibility gap at $T=0$ K closes at $x\sim 0.04$, i.e., the location of the minimum of that curve. This fact can be considered as the main consequence of the *ab initio* result giving a change in sign in the hof. The implications of this are as follows. Figure 3 shows how the phase diagram at low T and low x is modified if one considers the heat of formation predicted by *ab initio* calculations. This diagram is calculated using a classic potential that reproduces the energetics (in particular, the change in sign at some low Cr concentration), and by doing the thermodynamics exactly via switching Hamiltonians and thermodynamic integration techniques. The fact that the miscibility gap closes at finite x and that the maximum in the hof is higher than the SSOL value implies that the location of the *solvus* is significantly affected.

In summary, we observe that the change in sign of the heat of formation at about 6% Cr modifies the location of the *solvus* in the phase diagram by making it much steeper than the SSOL value. The solubility limit above ~ 700 K is much less than the value in SSOL and conversely, below ~ 700 K it is much higher. In particular, at low temperature, even at 0 K, there is a finite Cr solubility because the *solvus* does not go to $x_{\text{Cr}}=0$ at $T=0$ but to $x_{\text{Cr}}\sim 0.04$. As we pointed out above, the finite Cr solubility at 0 K is a result that is not affected by the controversy regarding the value of the hof around equiatomic composition. However, how steep the

solvus is at both ends of the diagram strongly depends on that value. The solubility of Fe in the α' phase, as we predict it, is too low compared to experiments⁵ and SSOL, a result also related to the high hof predicted *ab initio*.

This work was performed under the auspices of the U.S. Department of Energy by the University of California, Lawrence Livermore National Laboratory under Contract No. W-7405-Eng-48, with support from the Laboratory Directed Research and Development Program.

¹T. Massalski, in *Binary Alloy Phase Diagrams*, edited by William W. Scott, Jr. (American Society for Metals, Metals Park, OH, 1986), Vol. 1, p. 822.

²N. Saunders and A. P. Miodownik, in *CALPHAD: A Comprehensive Guide*, edited by R. W. Cahn (Pergamon, Oxford, 1998).

³J. O. Anderson and R. Sunderman, *CALPHAD: Comput. Coupling Phase Diagrams Thermochem.* **11**, 83 (1987).

⁴I. Mirebeau, M. Hennion, and G. Parette, *Phys. Rev. Lett.* **53**, 687 (1984).

⁵H. Kuwano and Y. Hamaguchi, *J. Nucl. Mater.* **155**, 1071 (1988).

⁶V. V. Sagaradze, I. I. Kositsyna, V. L. Arbizov, V. A. Shabashov, and Y. I. Filippov, *Phys. Met. Metallogr.* **92**, 508 (2001).

⁷V. A. Shabashov, A. L. Nikolaev, A. G. Mukoseev, V. V. Sagaradze, and N. P. Filippova, *Bull. Russ. Acad. Sci. Phys.* **65**, 1094 (2001).

⁸M. H. Mathon, Y. de Carlan, G. Geoffroy, X. Averty, and A. Alamo, *J. Nucl. Mater.* **312**, 236 (2003).

⁹M. Hennion, *J. Phys. F: Met. Phys.* **13**, 2351 (1983).

¹⁰P. Olsson, I. A. Abrikosov, L. Vitos, and J. Wallenius, *J. Nucl. Mater.* **321**, 84 (2003).

¹¹A. A. Mirzoev, M. M. Yalalov, and D. A. Mirzaev, *Phys. Met. Metallogr.* **97**, 336 (2003).

¹²P. Klaver (private communication).

¹³M. I. Mendeleev, S. Han, D. J. Srolovitz, G. J. Ackland, D. Y. Sun, and M. Asta, *Philos. Mag.* **83**, 3977 (2003).

¹⁴J. Wallenius, P. Olsson, C. Lagerstedt, N. Sandberg, R. Chakarova, and V. Pontikis, *Phys. Rev. B* **69**, 094103 (2004).

¹⁵A. Caro, D. A. Crowson, and M. Caro, *Phys. Rev. Lett.* **95**, 075702 (2005).

¹⁶E. O. Arregui, M. Caro, and A. Caro, *Phys. Rev. B* **66**, 054201 (2002).

¹⁷A. Caro, P. E. A. Turchi, M. Caro, and E. M. Lopasso, *J. Nucl. Mater.* **336**, 233 (2005).

¹⁸A. Caro, M. Caro, E. M. Lopasso, P. E. A. Turchi, and D. Farkas, *J. Nucl. Mater.* **349**, 317 (2006).

¹⁹E. M. Lopasso, M. Caro, A. Caro, and P. E. A. Turchi, *Phys. Rev. B* **68**, 214205 (2003).

²⁰A. Caro, M. Caro, E. M. Lopasso, P. E. A. Turchi, and D. Farkas, *J. Nucl. Mater.* **336**, 233 (2004).